Pathogens and Disease, 76, 2018, fty041

doi: 10.1093/femspd/fty041
Advance Access Publication Date: 19 April 2018
Research Article

RESEARCH ARTICLE

Biofilm-forming ability and infection potential of *Pseudomonas aeruginosa* strains isolated from animals and humans

Dusan Milivojevic[1,2], Neven Šumonja[3], Strahinja Medić[4], Aleksandar Pavic[1], Ivana Moric[1], Branka Vasiljevic[1], Lidija Senerovic[1] and Jasmina Nikodinovic-Runic[1,*,†]

[1]Institute of Molecular Genetics and Genetic Engineering, University of Belgrade, Vojvode Stepe 444a, 11000 Belgrade, Serbia, [2]Faculty of Veterinary Medicine, University of Belgrade, Bulevar Oslobodjenja 18, 11000 Belgrade, Serbia, [3]Centre for Multidisciplinary Research, Institute of Nuclear Sciences Vinca, University of Belgrade, Mike Petrovica Alasa 12–14, 11001, Belgrade, Serbia and [4]VetLab Ltd., Veterinary Laboratory for Clinical Diagnostics, Savska 31, 11000 Belgrade, Serbia

[*]**Corresponding author:** The Institute of Molecular Genetics and Genetic Engineering, University of Belgrade, Belgrade, Serbia. Tel: +381 11 3976034; E-mail: jasmina.nikodinovic@imgge.bg.ac.rs

One sentence summary: No significant differences between pathogenicity of *Pseudomonas aeruginosa* isolates from animal and human infections were detected, while pyocyanin-producing, biofilm-forming and hemolytic ability were highlighted as important predictors of their infection ability.

Editor: Thomas Bjarnsholt

[†]Jasmina Nikodinovic-Runic, http://orcid.org/0000-0002-2553-977X

ABSTRACT

Pseudomonas aeruginosa has been amongst the top 10 'superbugs' worldwide and is causing infections with poor outcomes in both humans and animals. From 202 *P. aeruginosa* isolates (n = 121 animal and n = 81 human), 40 were selected on the basis of biofilm-forming ability and were comparatively characterized in terms of virulence determinants to the type strain *P. aeruginosa* PAO1. Biofilm formation, pyocyanin and hemolysin production, and bacterial motility patterns were compared with the ability to kill human cell line A549 *in vitro*. On average, there was no significant difference between levels of animal and human cytotoxicity, while human isolates produced higher amounts of pyocyanin, hemolysins and showed increased swimming ability. Non-parametric statistical analysis identified the highest positive correlation between hemolysis and the swarming ability. For the first time an ensemble machine learning approach used on the *in vitro* virulence data determined the highest relative predictive importance of the submerged biofilm formation for the cytotoxicity, as an indicator of the infection ability. The findings from the *in vitro* study were validated *in vivo* using zebrafish (*Danio rerio*) embryos. This study highlighted no major differences between *P. aeruginosa* species isolated from animal and human infections and the importance of pyocyanin production in cytotoxicity and infection ability.

Keywords: *Pseudomonas aeruginosa*; biofilm; virulence factors; infection; animal isolates; human isolates

Received: 21 November 2017; **Accepted:** 18 April 2018

INTRODUCTION

Pseudomonas aeruginosa is an opportunistic pathogen that has remained on the 'top 10' common hospital 'superbugs' worldwide for more than a decade. Therapeutic options are still severely limited due to spread of antimicrobial resistant strains; thus, *P. aeruginosa* infection remains a life-threatening complication (Streeter and Katouli 2016). Serious *P. aeruginosa* infections, both acute and chronic, are often nosocomial and associated with compromised host defenses; however, this opportunistic pathogen is more and more recognized as the cause of disease in both livestock and companion animals, including otitis and urinary tract infections in dogs and cats, mastitis in dairy cows and goats, hemorrhagic pneumoniae in mink and foxes, and endometritis in horses (Kidd *et al.* 2011; Haenni *et al.* 2015). While phenotypic and genotypic characteristics of *P. aeruginosa* involved in enzootic or epizootic outbreaks of mastitis in bovine and small ruminants have been studied (Ohnishi *et al.* 2011; Scaccabarozzi *et al.* 2015), little attention has been given to *P. aeruginosa* strains isolated from infections of small companion animals.

At the time that it was sequenced, the genome of type strain *P. aeruginosa* PAO1 with 6.3 million base pairs was the largest bacterial genome sequenced; this sequence complexity provided insights into the basis of its versatility, environmental adaptability and intrinsic drug resistance and revealed an extensive repertoire of secreted virulence factors (Stover *et al.* 2000). Secreted virulence factors such as proteases, phospholipases, phenazines, rhamnolipids, exotoxins and endotoxins whose secretion is mediated by quorum sensing or cell-to-cell signaling guided research into pathogenicity of this strain (Vives-Florez and Garnica 2006; Hauser 2011; Oglesby-Sherrouse *et al.* 2014). Once an opportunistic pathogen like *P. aeruginosa* enters the host, its ability to cause infection has also been correlated with its tendency to form biofilms (Lee and Yoon 2017; Trøstrup *et al.* 2017). With the availability of more sophisticated technologies such as RNASeq and TnSeq that allowed for determination of the specific genes required for the optimal *P. aeruginosa* virulence in the murine model, a somewhat different picture emerged and some central metabolic genes came into focus including ones belonging to amino acid and vitamin biosynthetic pathways, suggesting that after all the usual virulence factors may not play such a pivotal role in the infection (Crousilles *et al.* 2015). From the wealth of available data, it can be concluded that pathogenesis of *P. aeruginosa* associated infections is highly multifactorial process and involves cell-associated factors as well as secreted virulence determinants (Lee *et al.* 2006; Olejnickova, Hola and Ruzicka 2014).

It is evident that complex relationships among *P. aeruginosa* virulence determinants have not been fully elucidated and particularly have not been comprehensively evaluated in population of animal isolates. Although *P. aeruginosa* has not been included in the recent literature overview of bacterial zoonoses transmitted by household pets, possibly due to limited literature data, small companion animals have been recognized as significant reservoir and carriers of microorganisms pathogenic for man, including methicillin-resistant *Staphylococcus aureus* (Loeffler and Lloyd 2010; Damborg *et al.* 2016). Given that close contact between household pets and people offers favorable conditions for bacterial transmission, we have assessed the biofilm formation ability and other virulence factors and the *in vitro* cytotoxicity of animal isolates predominantly from small companion animal infections of *P. aeruginosa* and compared them to that of isolates from humans, including the best characterized type strain *P. aeruginosa* PAO1. The potential to build a predictive model for the infection ability of this pathogen based on virulence determinants using an ensemble machine learning approach has also been addressed. The findings of the *in vitro* study have been validated in the *in vivo* zebrafish (*Danio rerio*) embryo infection model.

MATERIALS AND METHODS

Bacterial strains sources and identification

Pseudomonas aeruginosa PAO1 (NCTC10332) was obtained from the National Collection of Type Cultures (NCTC, Culture Collection of Public Health, Salisbury, UK).

The 202 strains, used in this study, were previously isolated and identified as *P. aeruginosa* using conventional microbiological methods (Pseudomonas Isolation Agar Base, HiMedia, Telangana, India) followed by biochemical (BBL Crystal enteric/non-fermenter ID kit, Becton, Dickinson and Company, Franklin Lakes, USA) from the specimens routinely delivered to Department for Microbiology, Faculty of Veterinary Medicine, Belgrade, Serbia; Regional Hospital Valjevo, Serbia; and Veterinary Laboratory 'VetLab', Belgrade, Serbia over 1-year period. From 202 strains, 121 were from animal specimens (dog n = 109, cat = 5, cow = 5, hamster n = 1, snake n = 1) and 81 from human specimens (Table 1). The strains were stored in a cryoprotective medium (Tryptic Soy Broth containing 20% (v/v) glycerol) at –70°C and for the test a fresh 24-h culture of particular strain was used.

All *P. aeruginosa* strains originating from human samples were collected from Regional Hospital Valjevo, Serbia, under ethical approval 01/8570. The analysis was performed retrospectively on isolates collected through routine clinical work and patient identifiable information was anonymized. The authors had no contact or interaction with the patients. Isolates were given unique codes, with 'A' within isolate name marking animal and 'H' human source of the isolate.

Molecular identification of selected isolates by 16S rRNA gene sequencing

Genomic DNA from isolated strains was extracted with the KAPA Express Extract Kit (Kapa Biosystems, Wilmington, USA). 16S rRNA gene was amplified from genomic DNA using universal bacterial primers 27F (5′-AGAGTTTGATCCTGGCTCAG-3′) and 1492R (5′-GGTTACCTTGTTACGACTT-3′). PCR amplification was performed in 2720 Thermal Cycler (Applied Biosystems, Waltham, USA) using the KAPA Taq PCR kit (Kapa Biosystems). Obtained PCR products were sequenced using the Applied Biosystems 3130 Genetic Analyzer (Applied Biosystems) and sequences were analyzed by the SeqMan Pro software (DNASTAR Inc., Madison, USA). The BLAST program (NCBI, http://www.ncbi.nlm.nih.gov) was used for sequences similarity search.

Alignment of sequences and homologous sequences taken from GenBank was performed with Clustal W 2.0 algorithm (https://www.ebi.ac.uk/Tools/msa/clustalw2/). A phylogenetic tree was constructed by the maximum-likelihood algorithm using the Jukes–Cantor distance correction included in MEGA7 package (Kumar, Stecher and Tamura 2016). The tree was rooted using 16S rRNA gene sequence of *Bacillus subtilis* B-1 (AB213262.1) as an outgroup.

Table 1. Distribution of *P. aeruginosa* isolates used in this study by type of sample from which they were isolated.

Origin of specimens	Ear swabs	Urine samples	Wound swabs	Skin swabs	Vaginal swabs	Eye swabs	Mouth swabs	Nasal swabs	Sputum samples	Milk samples
Animal 121	55	8	4	24	11	6	5	4	0	4
Human 81	12	30	8	4	4	1	1	0	21	0

Biofilm formation assays

Submerged biofilms

Biofilm quantification assays were performed in microtiter plate format using a crystal violet (CV) staining of adherent cells according to published protocols (Merritt, Kadouri and O'Toole 2005). Overnight cultures of *P. aeruginosa* strains were diluted to optical density (OD) OD600 of 0.2 and subcultured at 37°C in TSB medium (HiMedia Laboratories, Telangana, India) in a 96-well microtiter plates. After 24-h growth, planktonic cells were removed, wells were washed with PBS and biofilms fixed with 100 μL of 99% (v/v) cold methanol followed by staining with 0.1% (v/v) CV. After washing, CV was solubilized with 150 μL of glacial acetic acid (33%, v/v) and absorbance was measured at 550 nm using Tecan Infinite 200 Pro multiplate reader (Tecan Group Ltd, Männedorf, Switzerland). Assay was performed in hexaplicate and repeated three times.

Air–liquid biofilms

Air–liquid (A-L) biofilm assay was performed in polystyrene tubes (15 mL volume) as described previously (Olejnickova, Hola and Ruzicka 2014). Overnight cultures were diluted (OD600 of 0.2) and 0.2 mL of diluted cultures added to 1.8 mL of fresh TSB and further incubated at 37°C for 24 h. After incubation, cultures were discarded and polystyrene tubes were washed three times with PBS, adhered material fixed by air drying and stained with 0.1% (v/v) CV. Submerged biofilm was removed by adding 1.5 mL of glacial acetic acid (33%, v/v). The CV dye attached to the A–L biofilm was dissolved with 2 mL of acetic acid (33%, v/v). The tubes were vortexed for 30 s, and 150 μL of the solution was used for the absorbance measurement at 550 nm using plate reader (Tecan Group). The assay was performed for each strain in triplicate.

In vitro cell infections (cytotoxicity)

In vitro cell infection assay was performed for all bacterial isolates according to O'Loughlin *et al.* (2013) with minor modifications. Human lung carcinoma cells (A549) were obtained from the American Type Culture Collection (ATCC; Manassas, Virginia, USA). Cells were maintained as monolayer cultures in RPMI-1640 supplemented with 100 mg L^{-1} streptomycin, 100 U mL^{-1} penicillin and 10% (v/v) FBS (all from Sigma). Cells were grown in a humidified atmosphere of 95% air and 5% CO_2 at 37°C. Human A549 cells were grown in culture flasks (Sarstedt, Nümbrecht, Germany). Before infection, the A549 cells were treated with trypsin–EDTA (Sigma), split, counted and aliquoted into 96-well plates at 100 000 mammalian cells per well. Cells were grown for 20 h and then washed three times with PBS (Sigma) before bacterial suspension adjusted to final OD600 of 0.02 in 100 μL of RPMI containing 10 μg mL^{-1} propidium iodide (PI; Sigma) was added. PI fluorescence was measured every 2 h (excitation/emission (nm): 535/617) for 20-h period, using Tecan Infinite M200 pro plate reader. The fluorescence of PI measured at 10 h was used for the comparison of cytotoxicity of 40 different *P. aeruginosa* isolates. Appropriate controls such as bacteria in the absence of A549 cells as well as cells without addition of bacterial suspension were included in each experiment. The cytotoxicity was calculated according to formula:

$$\text{Cyt}(\%) = (\text{Fbact}/\text{Fdet})^{*}100$$

where Fbact represents cytotoxicity obtained in the presence of bacteria and Fdet represents fluorescence of non-infected cells lysed with 0.1% Triton-X100.

Fluorescent staining and microscopy

To visualize biofilm formation in the presence of human A549 cells and to distinguish between live and dead cells, three different nucleic acid stains were used: SYTO9 green fluorescent membrane permeable stain (ThermoFisher Scientific, Waltham, Massachusetts, USA), DAPI membrane permeable fluorescent dye (ThermoFisher Scientific) and PI red fluorescent membrane impermeable dye (Sigma, Munich, Germany). Briefly, 1 mL of RPMI medium containing 200 000 cells was placed in a 24-well microtiter plate containing the microscopic cover glass at the bottom (Sarstedt), and incubated for 24 h under previously described conditions. Overnight cultures of different bacterial isolates were washed with PBS and then adjusted to OD600 of 0.002 in 1 mL of RPMI containing 0.5% (v/v) of fetal bovine serum. Bacterial suspensions were then added to each well of a 24-well microtiter plate and after incubation for 8 or 16 h cells were washed three times with PBS, and stained with 300 μL PBS containing 2.5 μM SYTO9, 2.5 μM DAPI and 2.5 μM PI at room temperature for 30 min. Cells were then observed under a fluorescence microscope (Olympus BX51, Applied Imaging Corp., San Jose, California, USA) under ×20 000 magnification.

Motility assays

Swimming motility was measured according to previously described protocol (Ha, Kuchma and O'Toole 2014a,b). Overnight cultures were diluted to OD600 of 0.2 and by using toothpick bacteria were point-inoculated onto M8 plates (5 g L^{-1} Na_2HPO_4, 3 g mL^{-1} KH_2PO_4, 0.5 g L^{-1} NaCl, 0.2% glucose, 0.5% casaminoacids and 1 mM $MgSO_4$) containing 0.3% (w/v) agar. The plates were incubated for 18 h at 37°C. The distance of colony migration around the inoculation site was evaluated by measuring the diameter of the covered areas.

A swarming assay was performed on M8 plates containing 0.6% agar. Plates were inoculated with 2.5 μL of the diluted *Pseudomonas* cultures (OD600 of 0.2), and the phenotype was observed and measured after 16-h incubation at 37°C (Ha, Kuchma and O'Toole 2014a,b).

Twitching motility was evaluated as previously described (Olejnickova, Hola and Ruzicka 2014). Overnight *Pseudomonas* cultures were stabbed with a toothpick into LB plates supplemented with 1% agar and incubated overnight at 37°C for 20 h and incubation continued for additional 72 h at 25°C. Bacterial migration along the plastic surface was detected and measured

by CV (2%, (v/v)) staining after removing the agar from the plate (Olejnickova, Hola and Ruzicka 2014).

Hemolysin and pyocyanin production assays

Hemolytic activity assay was performed according to procedure described by Olejnickova *et al.* (2014) with minor modifications. *Pseudomonas aeruginosa* isolates were grown in TSB medium overnight at 37°C then OD600 was adjusted to 0.2, and 1 mL of the culture was mixed with 50 μL of pre-washed sterile sheep erythrocytes (Torlak, Belgrade, Serbia). After 3 h of incubation at 37°C, the debris was removed by centrifugation (20 min, 10 000 g, 20°C, Eppendorf 5145 D centrifuge, Hamburg, Germany), and the released hemoglobin was evaluated by measuring absorbance at 545 nm.

Pyocyanin production was evaluated by measuring OD of cell-free supernatant obtained by overnight *P. aeruginosa* cultures (O'Loughlin *et al.* 2013). Briefly, *P. aeruginosa* overnight cultures were incubated in TSB medium for 18 h then cells were separated from supernatant by centrifugation (20 min, 10 000 g, 20°C; Eppendorf 5145 D centrifuge). Cell-free supernatants were analyzed for pyocyanin using a Ultraspec 3300 pro (Amersham Biosciences, Little Chalfont, UK) spectrophotometer at 695 nm.

Statistical analysis

Data obtained for eight continuous attributes (phenotypic characteristics) describing 41 strains were regarded as data with non-normal distribution and the presence of outliers. For correlation analysis, robust rank correlation measure was used (Li *et al.* 2012). The R language was used for implementation of robust rank correlation in package 'rococo' (http://www.R-project.org/). 'Gauss' strict fuzzy ordering was used to define rank correlation coefficient. Correlations between attributes with robust rank correlation coefficient $\gamma \geq 0.3$ and $P < 0.05$ over 10 000 permutations were deemed to be significant (Bodenhofer and Klawonn 2008). Hierarchical clustering of 41 isolates based on similarity of eight attributes was executed in R. For visualization purposes, the package 'dendextend' was used (Galili 2015).

Predictive potential of seven phenotypic attributes in relation to the cytotoxicity was explored by non-linear regression analysis. For multivariable supervised modeling non-parametric state-of-the-art machine learning algorithm extreme gradient boosting (XGBoost) was used, which is implemented in R as 'xgboost' package (Chen and Guestrin 2016). XGboost is ensemble machine learning approach based on principle of boosting classification and regression trees. Highly robust to different kind of data and highly computational efficient, XGBoost is able to capture complex relations between predictor variables and outcome with high predictive efficiency. In order to decrease regression error of XGBoost models, the random XGBoost method hyperparameter space search was applied. For measure of predictive performance of the models, the leave-one-out cross-validation which is dictated by size of dataset has been used. The relative importance of each of the tested attributes in prediction of the cytotoxicity was extracted from XGBoost model.

Samples were grouped as animal and human and according to the type to swab and liquid (Table 1). To find out if there were differences between distributions of four groups, Mann–Whitney test (Wilcoxon Rank-Sum Test) implemented in R. In addition, the relative effect, also denoted as probabilistic index, was measured to explore attributes based on difference between groups of isolates (Kieser, Friede and Gondan 2013). The relative effect was used as implemented in R package 'npmv' (Burchett *et al.* 2017). In order to explore differences between groups of isolates based on combined effect of all variables, XGBoost as non-linear classificator was applied.

Maintenance and infection of zebrafish embryos

Wild-type zebrafish (*Danio rerio,* wt) embryo were kindly provided by Dr Ana Cvejic (Wellcome Trust Sanger Institute, Cambridge, UK) and raised to adult stage in our facility upon controlled temperature (28°C) and light (14:10-h light-dark photoperiod) conditions; fishes were regularly fed with commercially dry flake food (TetraMin flakes; Tetra Melle, Germany) twice a day and *Artemia nauplii* once daily. Embryos for the infection experiments were produced by the pairwise mating of adult fishes, collected and reared in petri dishes containing the embryos water (0.2 g L^{-1} of Instant Ocean Salt in distilled water) at 28.5°C.

Bacterial cells for microinjection into zebrafish embryos were prepared as previously described by Brannon *et al.* (2009). Briefly, the single colonies of each tested strain (for the validation of *in vitro* study, PAO1 and seven isolates were included: BU10A, BK6A, U31A, BR2A, S20H, BK25H and U24H) were inoculated into LB broth, grown overnight at 37°C with shaking (180 rpm), subcultured 1:100 in the same medium and grown to an OD600 of 0.7–0.8. To prepare final inoculum for injection, 2 mL of the log-phase bacteria was pelleted by centrifugation (1500 *g* for 5 min) (Eppendorf Centrifuge 5415D), washed twice with sterile PBS and finally suspended in PBS to achieve the desired OD.

At 24 h post fertilization (hpf), embryos were manually dechorionated and kept in the embryos water at 28.5°C. At 30–32 hpf, embryos were anesthetized by addition of tricaine-methane sulfonate (200 μg/mL) (Sigma-Aldrich, St. Louis, MO) and injected with bacterial cells (2 nL corresponding to 600–650 bacterial cells) into the yolk circulation valley as previously reported by Clatworthy et al. (2009), using a pneumatic picopump (PV820, World Precision Instruments, USA). The groups of 25–30 embryos were microinjected by each of eight selected strains. Injected embryos were returned to the embryos water, incubated at 28.5°C and monitored for survival at regular intervals up to 4 days post infection (dpi) under a stereomicroscope (SMZ143-N2GG, Motic, Germany). Dead embryos were removed daily. To determine the number of CFU microinjected in each set of embryos, bacteria were also microinjected in PBS and plated on LB agar.

In order to localize and visualize bacterial infection inside the embryos, prior to microinjection the PBS-washed bacterial cells were labeled with 10 μM solution of a CellTrackerTM Red CMTPX Dye (Molecular Probes, ThermoFisher Scientific) according to the manufacturer's instructions.

Kaplan–Meier survival curves were plotted in Microsoft Excel. Figure processing and assembly was performed using CorelDraw X7 and Photoshop CS2.

All experiments involving zebrafish were performed in compliance with the European directive 2010/63/EU and the ethical guidelines of Guide for Care and Use of Laboratory Animals of Institute of Molecular Genetics and Genetic Engineering, University of Belgrade.

RESULTS

Biofilm-forming ability and 16S relatedness of selected *P. aeruginosa* isolates

Sessile or biofilm mode of growth is seen as common cause of persistent bacterial infections. Chronic *P. aeruginosa* infections

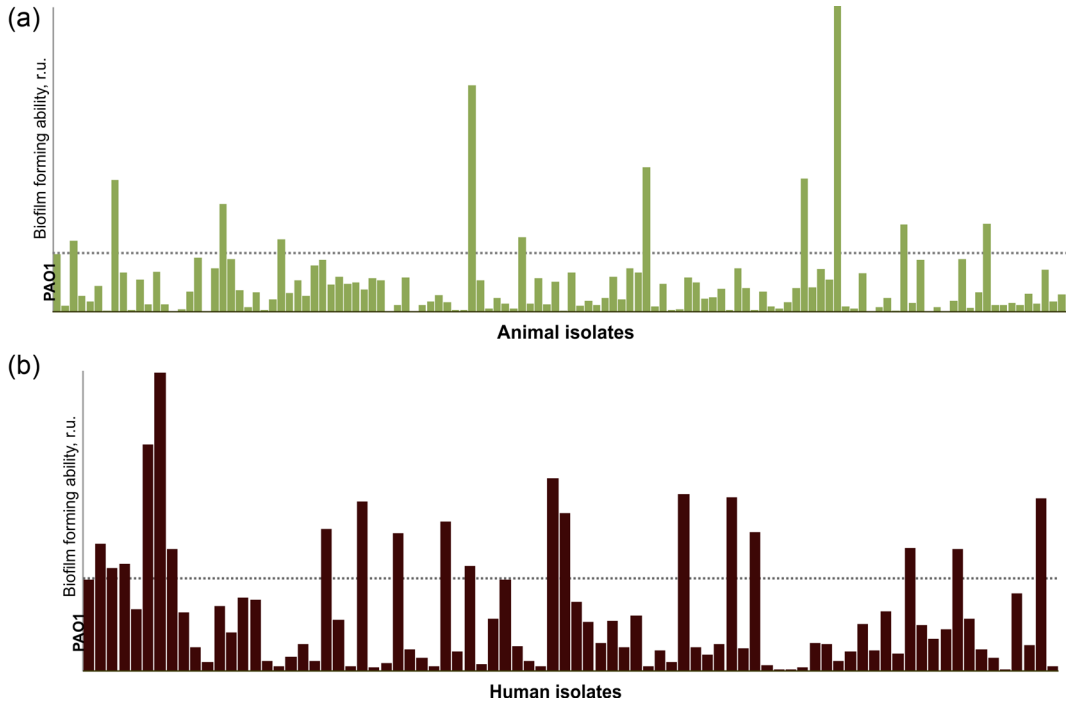

Figure 1. Total biofilm-forming ability of 202 *P. aeruginosa* spp. from (**a**) animal (n = 121) and (**b**) human (n = 81) specimens in relative units (r.u.) in comparison to type strain *P. aeruginosa* PAO1.

of small companion animals have generally received little attention. Nonetheless, based on the statistical data of the veterinary laboratory for clinical diagnostics VetLab (Belgrade, Serbia), they represent 3% of all tested samples (sample = identified bacterial isolate, with an average sample frequency of 150 per week). From these, 60% *P. aeruginosa* isolates were from ear swabs, 30% skin swabs and 10% originated from other samples such as urine or milk. We have collected 121 animal isolates over 1-year period and assessed them for the biofilm-forming ability. For the direct comparison, 81 isolates identified as *P. aeruginosa* were collected from Regional Hospital Valjevo (Valjevo, Serbia) (Table 1). Isolates were subjected to standard antibiotic susceptibility testing for Gram-negative bacteria at the time of isolation, and apart to intrinsic resistance characteristic of *P. aeruginosa*, no significant resistance was recorded (data not shown).

Submerged biofilm-forming ability has been assessed for 202 human and animal isolates of *P. aeruginosa* and compared to that of type strain PAO1 (Fig. 1). In total, 11 out of 202 isolates (5%) had no ability to form biofilms under tested conditions (8 animal and 3 human isolates). On the other hand, 30 out of 202 isolates (15%) had a greater ability to form biofilm than PAO1. Specifically, 11 out of 121 animal isolates (9%) and 19 out of 81 human isolates (23%) had this ability, with 10 of these 11 animal isolates originating from the swabs while 12 of these 19 human isolates originated from the fluid samples (Table S1, Supporting Information). Ear swabs of animals were the source of five very good biofilm producers, namely BU10A, BU22A, BU35A, BU69A and BU31A, with levels of up to 5-fold higher in comparison to PAO1 and they were all from the canine samples (ear swabs). On the other hand, 7 of 19 human good biofilm producers originated from sputum, specifically S2H, S19H, S20H, S22H, S25H, S26H, S27H with levels of up to 3-fold higher in comparison to PAO1.

Based on the biofilm formation assessment 40 isolates were brought forward for detailed analysis of virulence factors. Of these, 30 isolates (animal n = 11, human n = 19) had better ability to form biofilms in comparison to PAO1 (Table S1, Supporting Information) and 10 were selected as very poor biofilm producers (animal n = 8, human n = 2). From 40 selected, 25 isolates were from swabs samples (animal n = 18, human n = 7) and 15 isolates were from body fluid sources (animal n = 1, human n = 14).

The partial sequence of 16S rRNA (600 nt; 97%–100% identity to two *P. aeruginosa* type strains) was determined for these 40 isolates and from the phylogenetic tree it could be concluded that isolates were closely related and with animal and human isolates distributed evenly throughout the tree no apparent clustering was detectable (Fig. S1, Supporting Information).

Cytotoxicity in A549 human cell line and virulence factors of *P. aeruginosa* isolates

We have used *in vitro* infection of human A549 cell line assay as a measure of pathogenicity to compare 40 different *P. aeruginosa* isolates and to rank other virulence determinants of these strains using human type strain PAO1 as a reference. PAO1 has been assigned as moderately pathogenic strain in various infection models, including *Caenorhabditis elegans*, *Galleria mellonella* and mice, and less virulent than *P. aeruginosa* PA14 (Mahajan-Miklos *et al.* 1999; Lee *et al.* 2006). Cytotoxicity of different *P. aeruginosa* isolates was compared to PAO1 upon 10 h of infection (Table S2, Supporting Information; Fig. 2a). Both animal and human isolates showed similar infection potential levels of cytotoxicity with ~50% of isolates from both groups causing more cell death then PAO1. However, among isolates with two or more times higher cytotoxicity in comparison to PAO1, 35% were animal and 65% human isolates (Figs 2a and 4b). The highest *in vitro* cell killing among animal isolates was observed for BU10A (isolated from ear swab of a dog) inducing 49% cell death (Table S2, Supporting Information). The most cytotoxic human

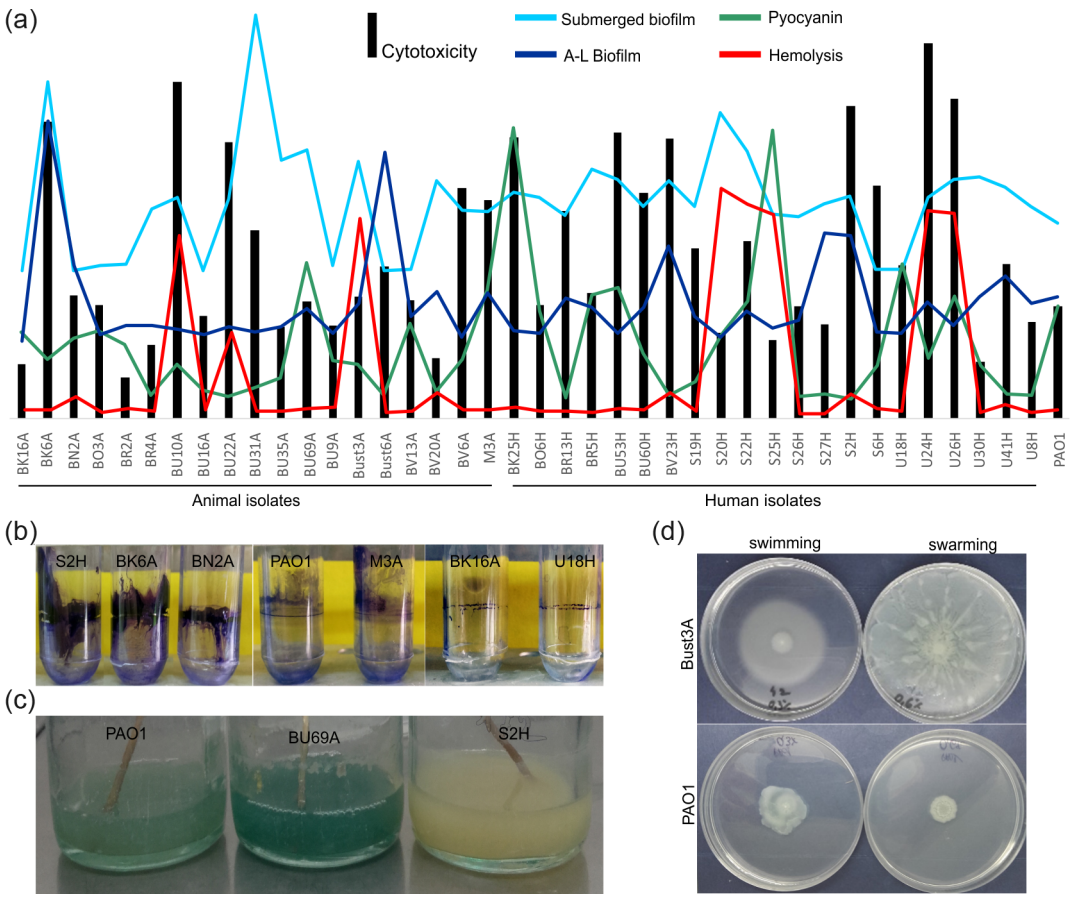

Figure 2. Phenotypic characteristics of *P. aeruginosa* isolates in comparison to PAO1 type strain: (**a**) submerged biofilm and air–liquid biofilm formation, pyocyanin and hemolysin production in comparison to cytotoxicity; (**b**) A-L biofilm formation of S2H, BK6A, BN2A, M3A, BK16A and U18H; (**c**) pyocyanin production of BU69A, S2H and (**d**) motility (swarming and swimming) of strain Bust3A. Designation 'A' within isolate name marks animal and 'H' human source of the isolate.

strain was U24H from urine sample which killed 55% of cells (Table S2, Supporting Information). The least cytotoxic isolates were BR2A and U30H, isolated from wound swab of a dog and human urine sample, causing 6% and 8% cell death, respectively (Table S2, Supporting Information).

Phenotypically, 40 isolates have been comprehensively evaluated for the biofilm formation (submerged and air-liquid), pyocyanin and hemolysin production, and motility patterns. Submerged and A-L biofilms were observed in all 40 strains (Fig. 2a). Overall, 12 isolates (30%) exhibited submerged biofilm-forming potential at least two times greater than PAO1, and 3 (25%) out of these 12 isolates showed cytotoxicity greater than 30%, while 6 isolates (15%) exhibited high ability to produce A-L biofilms, and half of those showed cytotoxicity greater than 30%.

The average submerged biofilm formation ability was not significantly different in animal in comparison to human isolates, with the highest ability to form submerged biofilms determined for two animal isolates, BK6A and BU31A that was 3 and 4-fold higher in comparison to that of PAO1. Indeed, the cytotoxic effect of these two strains has been 2- and 1.6 -fold higher in comparison to that of PAO1. The progression of cell killing was observed by fluorescence microscopy at 8 and 16 h of infection (Fig. 3). Isolate BU31A formed biofilm aggregates on A549 cell layer already at 8 h of infection. The similar observation was made for U24H, the isolate with similar submerged biofilm-forming ability as PAO1, but 3.3-fold higher cytotoxic effect (Fig. 2a). At 16 h, BU31A biofilms covered almost the whole A549 cell layer. Biofilm formed by U24H could be observed scattered over the whole A549 cell layer but it appeared less confluent than biofilm formed by BU31A, although both isolates induced comparable cell death as detected by PI staining (Fig. 3). Phenotypically, these two isolates (BU31A and U24H) differed the most in the swimming ability with U24H being amongst the best swimmers (Fig. S2, Supporting Information). Isolate BK25H, as one of the highest pyocyanin producers, demonstrated similar potential to form biofilms on A549 cells as PAO1 at 8 and 16 h of cell infection; however, consistent with the data obtained for cytotoxicity, PI staining of BK25H-infected cells was more prominent than the cells infected with PAO1 during the same period.

The average ability to form A-L biofilms was not different amongst animal and human isolates. While animal Bust6A, BK6A, BN2A and human S2H, S27H, BV23H exhibited 1- to 3-fold higher ability to form A-L biofilm in comparison to PAO1, only S2H, BK6A and BV23H were almost three times more pathogenic in comparison to PAO1. BN2A and S27H did not show increased cytotoxicity in comparison to PAO1. Interestingly, the highest submerged biofilm-forming isolate BU31A showed comparable A-L biofilm production to PAO1, and 1.6-fold increased cytotoxicity to PAO1 (Figs 2a and 3). Isolate U24H showed comparable biofilm-forming ability to PAO1, while its cytotoxicity was 3-fold higher in comparison to PAO1 (Fig. 2a, Table S2, Supporting Information). This indicates that biofilm-forming ability was not quite a predictable factor of the cytotoxicity of certain *P. aeruginosa* strains.

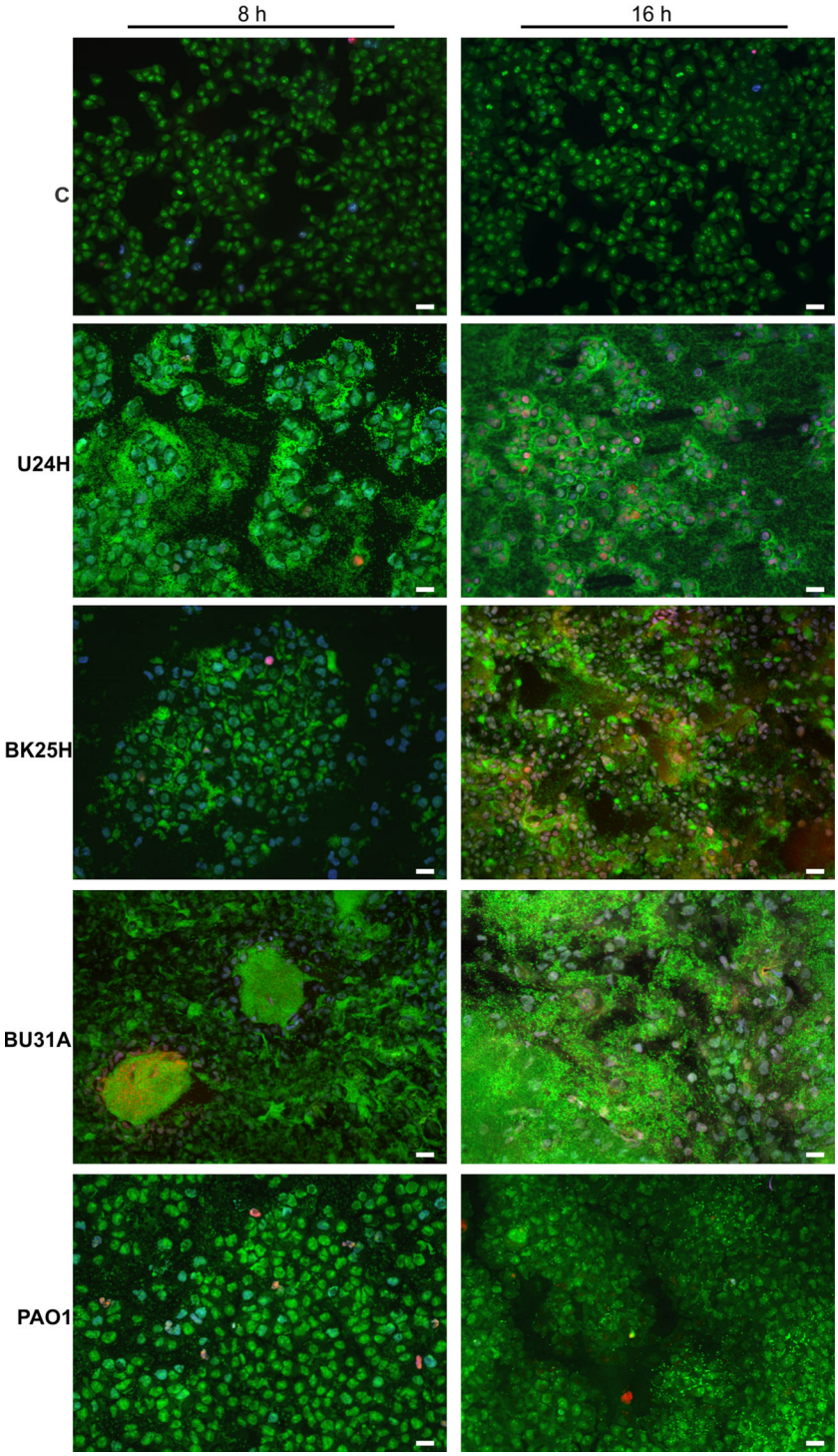

Figure 3. *In vitro* infection of A549 cell line using *P. aeruginosa* isolates U24H, BK25H, BU31A and PAO1. After incubation for 8 or 16 h, the nuclei of A549 cells were stained with DAPI (blue), live bacteria and A549 cells were labeled with SYTO9 (green), while dead bacteria and A549 cells were stained with PI (red). Extracellular DNA within biofilm was stained with SYTO9 and PI and appeared orange. Control represents A549 cells without bacteria. Scale bars represent 10 μm.

The blue-green pigment pyocyanin (1-hydroxy-5-methyl-phenazine) gives *P. aeruginosa* spp. their distinct color (Fig. 2c). The average pyocyanin production ability was significantly higher ($P < 0.001$) in human in comparison to animal isolates (Fig. 2a); however only four isolates (10%; BU69A, BK25H, S25H and U18H) produced significantly more pyocyanin in comparison to PAO1. Of these only one isolate, BK25H, showed significant cytotoxic effect. This isolate showed comparable biofilm production to PAO1.

Hemolysins cause host tissue damage during *P. aeruginosa* infection, and out of 40 isolates 10 (25%) exhibited higher hemolytic potential than PAO1, with 5 of those exhibiting high cytotoxicity on A549 cells (Fig. 2a). On average, hemolysis was significantly higher ($P < 0.001$) in human in comparison to

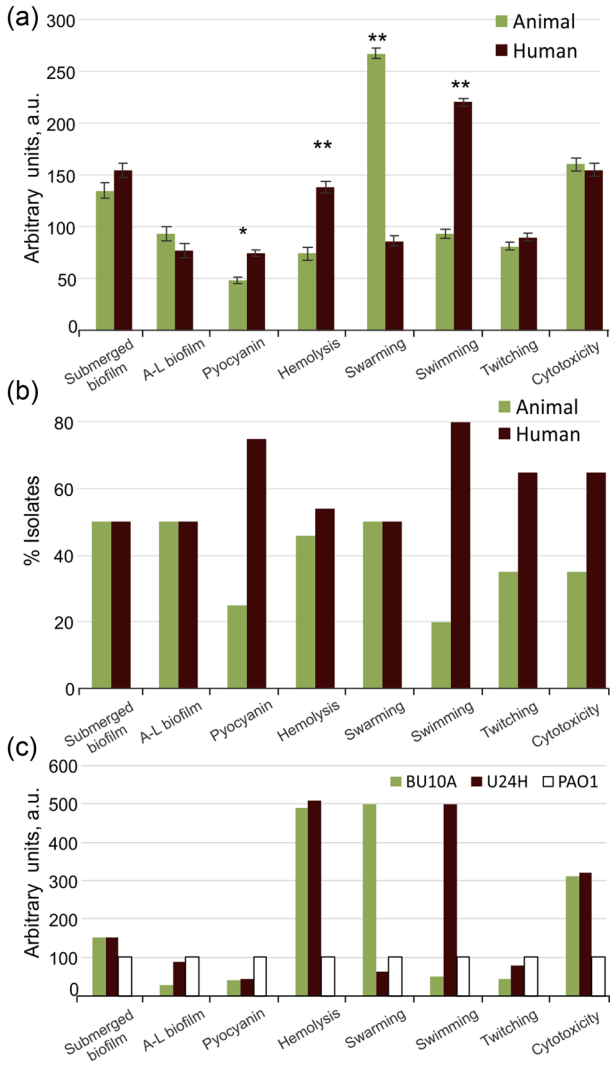

Figure 4. Comparison of phenotypic characteristics and the infection ability of *P. aeruginosa* animal and human isolates. (a) Average values for phenotypic characteristics between animal and human isolates. Error bars represent the standard error of the mean (*$P < 0.01$ and ** $P < 0.001$). (b) Distribution of significant producers of certain virulence factors among animals and human isolates. (c) Values for the two most pathogenic isolates in comparison to PAO1.

animal isolates; however, the highest hemolysis (20-fold higher in comparison to PAO1) was similar for five human isolates (S20H, S22H, S25H, U24H and U26H) and two animal isolates (BU10A and Bust3A). It is noteworthy that the highest submerged biofilm producer BU31A (isolated from dog ear swab) as well as high pyocyanin producer BK25H (isolated from human skin swab) showed markedly lower hemolysis in comparison to PAO1.

Motility assessment showed that on average animal isolates showed significantly higher swarming ability, while human isolates performed significantly better in the swimming assay ($P < 0.001$) (Fig. 4a). On average, significant difference was observed between animal and human isolates in twitching; however, distribution of isolates showing the highest ability to twitch was higher for human isolates (Fig. 4b). Swimming assessment showed that 12 isolates had significantly higher ability to swim than PAO1, 4 of them (10%) being animal and 8 (20%) being human isolates. The highest swimming activity was observed for BU53H and BK25H isolated from human ear swab and human skin swab, respectively. At the same time, these isolates showed very high cytotoxic effect. Consistently, the highest swimming activity was detected for U24H and U26H, which showed the highest cytotoxicity amongst human isolates. In general, 40% of those that exhibited good swimming ability showed higher cytotoxicity than PAO1. On average, animal isolates showed better swarming ability, but half of the isolates from both sources showed higher swarming ability than PAO1 (Fig. 4a and b). The most potent swarmer strain was animal isolate Bust3A from snake's mouth swab showing 30 times bigger motility zone than PAO1; it also showed considerable swimming ability, but caused similar cell killing as PAO1 (Fig. 2d and Fig. S2, Supporting Information). Most of the isolates demonstrated bigger twitching zones than PAO1, with 35% of them from animal and 65% from human samples (Fig. 4a and b). Three of the isolates with better twitching motility (15%), namely BU31A, S22H, S6H, also showed higher cytotoxic effect in comparison to PAO1.

From the qualitative observations, hemolysis and the high swimming ability were the most reliable predictors of high pathogenicity of *P. aeruginosa* isolates. The most pathogenic animal isolate BU10A was remarkably potent in hemolysis and swarming and had considerable submerged biofilm-forming ability, while the most pathogenic human isolate,U24H was remarkably potent in hemolysis and swimming and had considerable submerged biofilm-forming ability (Fig. 4c).

Non-parametric correlations between virulence factors and phenotypic clustering

Since robust ranking correlation is efficient for identification of non-linear relation between data that do not have normal distribution and are subjected to outliers, this statistical approach was used for analysis/identification of correlation between eight phenotypic characteristics (i.e. continuous attributes) determined for 41 *P. aeruginosa* stains (Fig. 5a). The structure of *in vitro* phenotypic data showed non-parametric properties and it was subjected to outliers. In general, under these conditions, correlations, either positive or negative, were not strong. The highest positive correlation was determined between hemolysis and the swarming ability, while the highest negative correlation was determined between A-L biofilm formation ability and swarming (Fig. 5a). The cytotoxicity (an indicator of the infection ability) was positively correlated with hemolysis and moderately negatively with the swimming ability. The tree of hierarchical clustering of 40 isolates and PAO1 based on eight different phenotypic characteristics (attributes) depicts no clustering (Fig. 5b). Three main branches were observable; however, animal and human samples were evenly distributed, with the isolates showing the highest cytotoxic effect, found within each branch. Interestingly, from this analysis the closest to type PAO1 strain was animal BU69A isolate showing similar cytotoxicity and other virulence factors, but higher pyocyanin production ability (Fig. 2a).

To evaluate predictive relation of seven phenotypic characteristics as explanatory attributes with the cytotoxicity (the infection ability indicator), the non-linear regressor XGBoost was applied. Given that the size of available data is crucial for learning process of any machine learning algorithm, the LOOCV train/test validation scheme has been applied. Using the LOOCV train/test scheme, the models' average performance in prediction of cytotoxicity of isolates was 7.64906 ± 2.726 root mean square error, indicating moderate efficiency of the prediction. It is noteworthy that although the models were

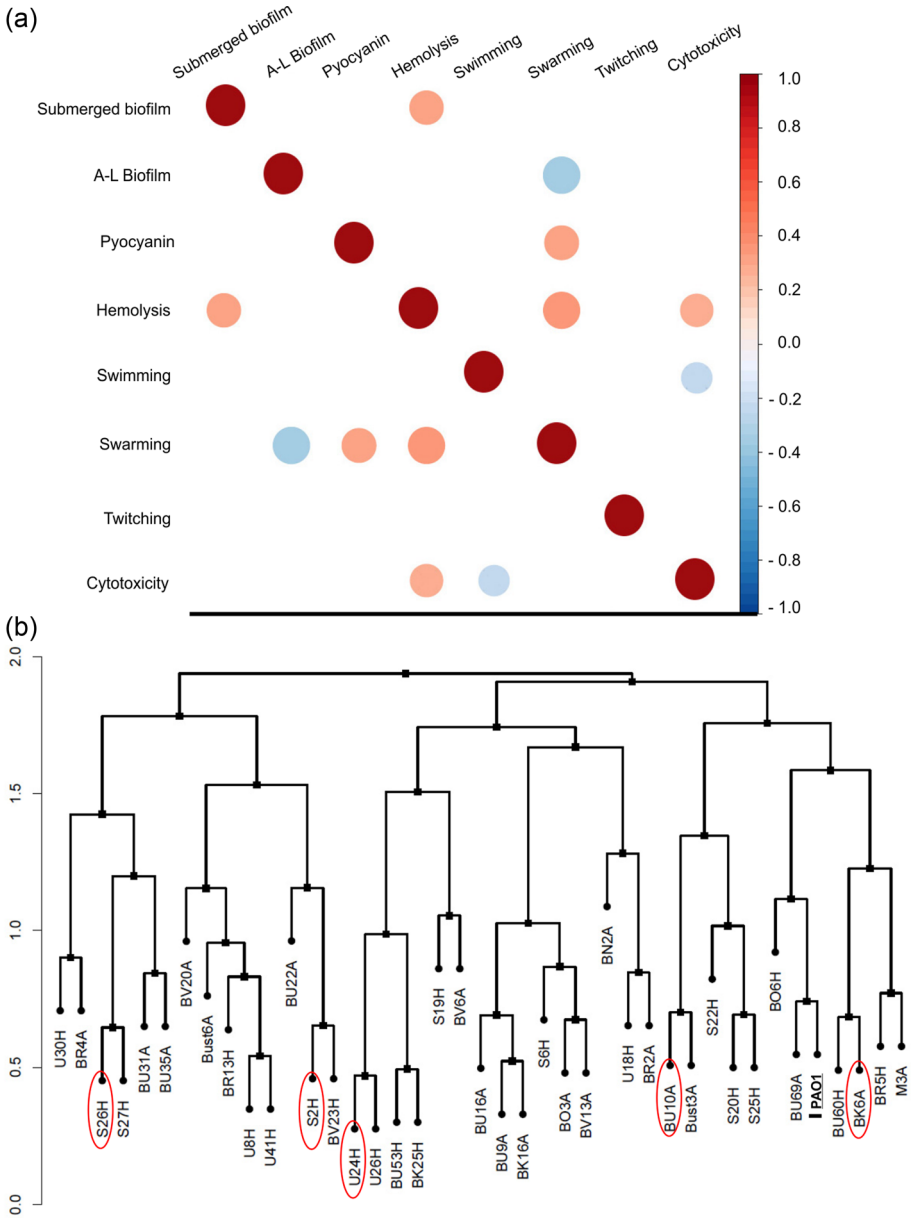

Figure 5. Statistical correlations between eight different attributes (**a**) and hierarchical clustering (**b**) of 40 *P. aeruginosa* isolates and type PAO1 strain. Isolates showing the highest cytotoxicity levels are circled, with PAO1 strain underlined. The $\gamma \geq 0.3$ and $P < 0.05$ over 10 000 permutations were considered to be significant.

moderately efficient in prediction of cytotoxicity of isolates the potential to further explore this approach with larger datasets is evident.

In contrast to qualitative observations, whereby hemolysis and the swimming ability were the best predictors of the cytotoxicity (Figs 2a and 4), based on the predictive model built by the XGBoost algorithm, the submerged biofilm formation showed the highest relative importance in predicting the cytotoxicity, followed by 1.5-fold lower relative importance of pyocyanin production, swimming ability and hemolysis (Fig. 6).

Statistical differences between groups of isolates

In order to determine if there were statistically significant differences between groups of isolates (animal versus human and isolates originating from swabs versus ones originating from fluid samples), two different approaches were used.

Initially, animal/human and swabs/fluid data sets were tested using the Wilcoxon rank-sum test and relative effect test, with all eight phenotypic characteristics tested in non-signed pairs (pairwise) from animal/human and swab/fluid data sets. Differences from both groups were not statistically significant under $P < 0.05$. The smallest P value and the biggest difference between animal/human groups were found in the cytotoxicity, followed by submerged biofilm formation and A-L biofilm formation. On other hand, the most significant difference between swab and fluid isolates was in A-L biofilm formation, followed by swimming and twitching ability (Table 2). Values obtained in this test also indicate that there is 62.9% probability that human isolate has higher cell-killing effect than any other isolate. Similarly, there is higher chance that isolate from fluid samples is

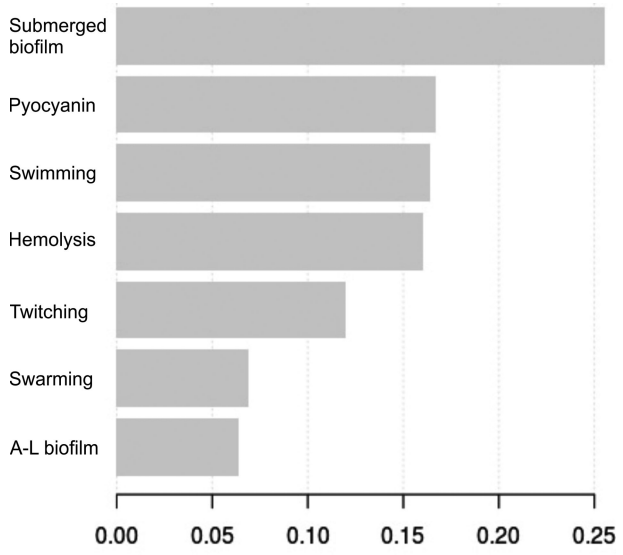

Figure 6. Relative importance of different virulence factors for prediction of the cytotoxicity as an indicator of infection ability obtained from the XGBoost regression model.

better in A-L biofilm formation than any other isolate from both groups (Table 2).

In addition to pairwise analysis of groups' differences, the multivariable non-linear machine learning XGBoost algorithm was also employed in the attempt to separate the groups based on the combined effect of eight phenotypic parameters. To evaluate classificatory ability to separate animal/human and swab/fluid groups receiver operator area under curve (AUROC), area under precision operator curve (AUPRC) and balanced accuracy (BA) performance metrics were used. AUROC and BA are highly sensitive to imbalanced classes in two datasets (i.e. different number of isolates belonging to human class in comparison to animal class, and the same for swab/fluid dataset). Ten-fold cross-validation (CV-10) classification results for animal/human datasets were AUROC = 0.62, AUPRC = 0.588 and BA = 59.56%. Therefore, separation between animal and human isolates was not very efficient, with BA being close to random. However, the algorithm more efficiently separated group swab from fluid, with result from CV-10: AUROC = 0.767, AUPRC = 0.771 and BA = 66%.

Analysis of *P. aeruginosa* infection in zebrafish (*Danio rerio*)

In order to validate *in vitro* study, systemic infection of zebrafish embryos was established by microinjection of selected *P. aeruginosa* individual bacterial isolates directly into the bloodstream in the yolk circulation valley at 30–32 hpf and embryos were monitored for 4 days (Fig. 7). In addition to PAO1, isolates that were selected for *in vivo* assay included ones that were the most cytotoxic (U24H and BU10A), the highest pyocyanin producer also being the one with the best swimming ability (BK25H), the highest A-L and high submerged biofilm producer (BK6A), the isolate with the highest hemolysis effect and high submerged biofilm producer (S20H), the highest submerged biofilm producer and with the best twitching ability (BU31A) and BR2A causing the least cytotoxic effect and performing poor in most other phenotypic assays (Fig. 2 and Fig. S2, Supporting Information).

According to the mortality rate scored at 4 dpi, the tested strains were ranked by virulence as follows: BK25H > BK6A > S20H > PAO1 > BU31A ≈ BR2A > BU10A ≈ U24H killing embryos between 73% and 23% (Fig. 7a). All strains except BK6A mostly killed the embryos within the first dpi, stage during which embryos are not fully immunocompetent (Fig. 7a). While the mortality rates remained relatively constant per each isolate, BK6A drastically reduced embryo survival at 4 dpi and it was distributed throughout whole zebrafish body with accumulation in the caudal region (Fig. 7b). Notably, PAO1, S20H and BK6A caused the severe tissue necrosis and the circulation retardation in the tail of infected embryos which extended to other tissue, alongside an appearance of pericardial edema, whole body edema and the swim bladder absence up to 4 dpi (Fig. S3, Supporting Information). On the other hand, the moribund embryos infected with other strains mostly showed damages in the yolk sac region (data not shown). In addition, embryos infected with BK6A were paralyzed at 3 dpi onward, suggesting that this strain or its toxic product(s) could target muscles and/or nerve tissues (data not shown).

DISCUSSION

Pseudomonas aeruginosa causes infections of both medical and veterinary significance. It is the fifth most frequent pathogen worldwide, the third in urinary infections and the seventh pathogen responsible for sepsis (Lister, Wolter and Hanson 2009). The wealth of knowledge regarding this important opportunistic pathogen is mostly coming from the human medical research. The management of *P. aeruginosa* infections poses a great challenge for both veterinarians and medical doctors because of the tendency of long persistence and spreading from subclinically infected individuals, and due to the intrinsic resistance as well as limited number of effective therapeutic options (Gellatly and Hancock 2013).

Frequency of isolation of this *P. aeruginosa* in companion animals is not well documented, but it appears that it is on the rise, especially in dogs (Petersen *et al.* 2002; Hillier *et al.* 2006). Reviewing the records of the veterinary clinical diagnostics laboratory (VetLab, Belgrade, Serbia) over 7-year period (2009–2016), it was determined that they represent 3% of all identified bacterial isolates, with the majority isolated from skin and ear swabs of dogs.

Table 2. Values (k) obtained in relative effect statistical test for pairwise comparison of phenotypic attributes of groups of isolates.

Group[a]	Submerged biofilm	A-L biofilm	Pyocyanin	Hemolysis	Swimming	Swarming	Twitching	Infection
A	0.39097[b]	0.42983	0.49624	0.49874	0.51002	0.50878	0.45739	**0.37093**
H	0.60903	0.57017	0.50376	0.50126	0.48998	0.49122	0.54261	**0.62907**
S	0.46667	**0.39467**	0.52800	0.46667	0.40267	0.56133	0.41067	0.47210
F	0.53333	**0.60533**	0.47200	0.53333	0.59733	0.43867	0.58933	0.52810

[a]A = animal; H = human; S = swab, F = fluid.
[b]Value k represent probability that randomly chosen isolate from any group has a higher value for certain characteristic then isolate randomly chosen from any other group.

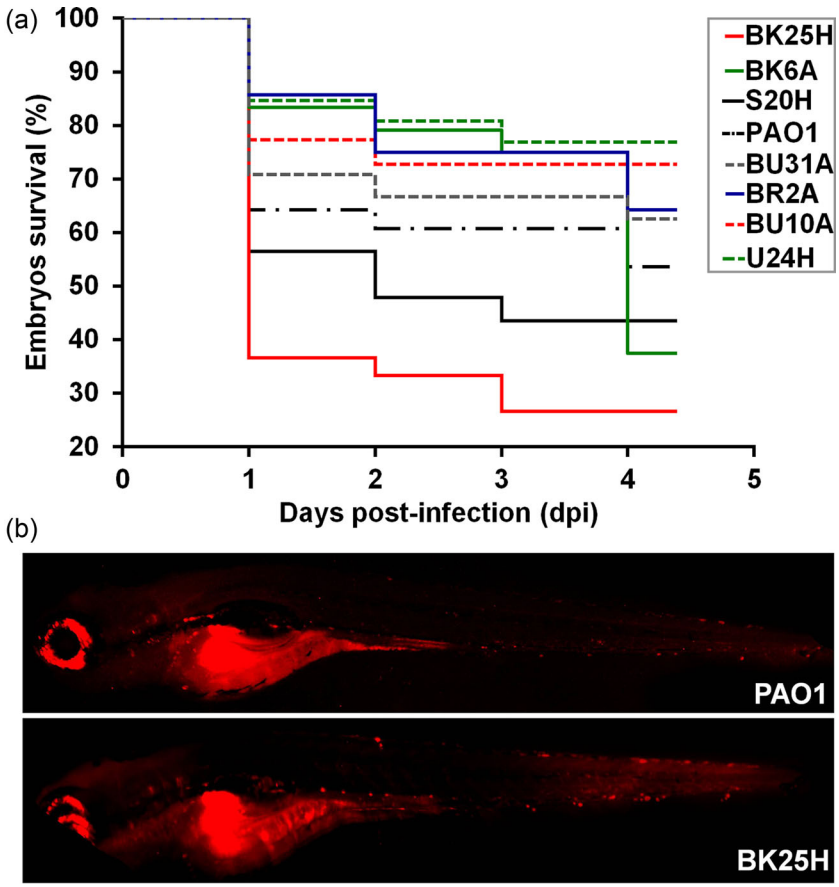

Figure 7. *In vivo* infection of 30–32 h post fertilization old zebrafish embryos with different *P. aeruginosa* isolates. (**a**) The Kaplan-Meier survival curves following infected embryos at regular intervals up to 4 days post infection. Data are representative of three replicates with 25–30 embryos/group in each replicate. (**b**) The bacterial cells distribution within infected zebrafish embryos. *Pseudomonas aeruginosa* isolates were labeled with CellTracker Red Fluorescent CMTPX Dye (Molecular Probes). The red fluorescence of zebrafish eyes is artifact.

This is in line with reports from the Michigan State University's Animal Health Diagnostic Laboratory reporting that *P. aeruginosa* was isolated from 7.5% and 27.8% of canine skin and ear samples, respectively, over a 6-year period (1992–1997; Petersen *et al.* 2002), and it was suggested to be a primary skin pathogen in dogs (Hillier *et al.* 2006).

Pseudomonas aeruginosa exhibits many different phenotypes *in vitro*, but the relative relationships between these phenotypes and failure to eradicate *P. aeruginosa* have not been well characterized (Lee *et al.* 2006; Crousilles *et al.* 2015). A wide range of pathogenic potential and virulence factors, such as adhesins, proteases, phenazines and exotoxins, have been well documented for *P. aeruginosa* clinical isolates. Furthermore, differential presence or expression of virulence factors has been shown to significantly impact disease severity and mortality in human infections. However, the complex relationships among virulence determinants have not been fully elucidated and very little is known about the structure of the *P. aeruginosa* population from diseased animals. Therefore, the aim of this study was to extend the current knowledge within the field by direct comparison of phenotypic characteristics and the infection ability of *P. aeruginosa* animal and human isolates and to assess the possibility of utilization of the state of the art ensemble machine learning approach in order to build a predictive model for the pathogenicity of this bacterium.

Sessile or biofilm mode of growth is seen as common cause of persistent bacterial infections. Chronic infections are usually associated with biofilms and increased antibiotic resistance, while acute infections have been connected with *P. aeruginosa* planktonic cultures (Gellatly and Hancock 2013). During the initial screen of 202 isolates, it was determined that 93% (113/121) of animal and 96% (78/81) of human isolates had the ability to form biofilms *in vitro* (Fig. 1). This high incidence of biofilm formation is known for human clinical isolates whereby it was 80%–88% in population of catheter-related infections (Olejnickova, Hola and Ruzicka 2014); however, this ability has been less studied in population of animal isolates. The importance of biofilm formation in bacterial pathogens of veterinary importance has been recognized, with *P. aeruginosa* described to produce extrapolymeric substance wherever conditions are appropriate for bacterial colonization leading to establishment of resistant infections (Gellatly and Hancock 2013). The biofilm-forming ability was found in 40% (33/83) of isolates from dogs with otitis and was suggested to play a role in the pathogenesis of the disease and to lead to the lack of response to treatment (Pye, Yu and Weese 2013). We also found that 9% (11/121) of animal isolates in comparison to 23% (19/81) of human isolates had better biofilm-forming ability than the best characterized PAO1 type strain regarded as moderately pathogenic (Lee *et al.* 2006). Given the established importance of biofilms in infection process, we have selected all of isolates

(n = 30) with the better ability to form biofilms than PAO1 and the poorest biofilm producers (n = 10) in order to relate their cytotoxicity with other phenotypic characteristics and expression of virulence factors. In addition to biofilm-forming ability, the production of pyocyanin has been shown to be involved in infection process by disrupting electron transport and inducing oxidative stress to the host (Lau *et al*. 2004). On the other hand, hemolysins cause host tissue damage during *P. aeruginosa* infection, and it has been suggested that high levels of hemolysins production *in vitro* could be used as surrogate information for assessing pyelonephritic potential of *P. aeruginosa* (Mittal *et al*. 2010). Motility (twitching, swimming, swarming or sliding) is strongly associated with the pathogenesis of *P. aeruginosa* as it enables this bacterium to colonize different environments (Arora *et al*. 2005).

In this study, significant cytotoxicity determined in the cell infection assay was exhibited by 34% of selected isolates (14/40). On average, there was no significant difference between levels of animal and human isolates' cytotoxicity, while human isolates produced higher amounts of pyocyanin, hemolysins and showed increased swimming ability. The ability to form biofilms was comparable between animal and human groups, while swarming ability was significantly higher in animal isolates. Similarly, there was no difference in the virulence between the groups of environmental and clinical strains of *P. aeruginosa* tested on *Drosophila melanogaster* and *Lactuca sativa* pathogenicity models (Vives-Florez and Garnica 2006). The acute infection ability of *P. aeruginosa* isolates from a hydropathic facility was similar to that of clinical isolates from respiratory infections in *Galleria mellonella* model (Pereira *et al*. 2014). Previously, *P. aeruginosa* isolates from dairy goats in Italy were shown to exhibit similar levels of virulence and pathogenic potential in comparison to environmental samples (Scaccabarozzi *et al*. 2015). To the best of our knowledge, this is the first report of the direct comparison of *P. aeruginosa* isolates from animal and human infections in terms of the infection potential levels of cytotoxicity and expression of virulence factors, showing comparable levels of the cell-killing ability of the two groups.

Overall, each isolate showed a unique pattern of production/expression of virulence-related phenotypes (Fig. 2 and Fig. S2, Supporting Information), making it difficult to infer correlations between the levels of certain virulence determinants, pathogenic potential and the source of isolation. No apparent clustering of isolates has been observed on dendrograms of both 16S rRNA partial sequence (Fig. S1, Supporting Information) or phenotypic characteristics (Fig. 5b). It is generally accepted that the *P. aeruginosa* population is non-clonal, and that population structure of *P. aeruginosa* is highly diverse with a high number of clonal groups with no or poor association between clonal groups and ecological niches or specific diseases (Haenni *et al*. 2015). Consistent with our study, high phenotypic as well as genotypic diversity has been previously observed for various *P. aeruginosa* isolates (Scaccabarozzi *et al*. 2015; Wright *et al*. 2015). Nevertheless, characterization of 33 isolates (7 from goat milk and 26 environmental isolates) revealed five major phenotypic clusters with correlation threshold of 22.34%, which was different to our study.

Based on the qualitative data, hemolysis and the high swimming ability were the most related to high cytotoxicity of *P. aeruginosa* isolates from this study (Fig. 2 and Fig. S2, Supporting Information), while a non-parametric statistical analysis confirmed a positive correlation with hemolysis and indicated moderate negative correlation with the swimming ability (Fig. 5a). In the already mentioned retrospective study of the isolates from dairy goats and surrounding environment (Scaccabarozzi *et al*. 2015), hemolysis and the biofilm-forming ability correlated positively which was consistent with our findings (Fig. 5a). In their study, hemolysis correlated positively with swimming, while we found positive correlation between hemolysis and swarming. On the contrary, phenotypical characterization of *P. aeruginosa* isolates from catheter-related infections revealed negative correlation between hemolysis and the submerged biofilm formations (Olejnickova, Hola and Ruzicka 2014). Negative correlation was reported between pyocyanin production and biofilm formation (Olejnickova, Hola and Ruzicka 2014), as well as pyocyanin and the swimming ability (Scaccabarozzi *et al*. 2015). In our study, pyocyanin production was positively correlated with the swarming ability (Fig. 5a). There are multiple contradictory reports of the correlation of certain phenotypic characteristic related to virulence factors in this pathogen with genetic evidence offered for the positive correlation of biofilm formation and twitching motility in strains isolated from ovine mastitis (Wright *et al*. 2015), as well as negative correlation between biofilm and pyocyanin production (Fernandez-Pinar *et al*. 2011). Analysis of the infection ability of *P. aeruginosa* isolates in zebrafish model confirmed that selected isolates could indeed proliferate and kill zebrafish embryos to different extent (Fig. 7). The highest killing efficiency was observed for two isolates with the highest pyocianin-producing ability (BK25H and BK6A). The production of pyocyanin was previously shown to play an important role in an acute zebrafish embryos infection with *P. aeruginosa* PA14, while biofilm formation and the production of elastase and alginate did not play a role in the infection (Chand *et al*. 2011). Interestingly, BK6A was the best biofilm producer and embryos infected with this isolate were paralyzed at 3 dpi onward, suggesting that this strain or its toxic product(s) could target muscles and/or nerve tissues, as previously reported for PAO1 strain (Llamas *et al*. 2009). The isolate S20H, with 20-fold higher hemolytic ability in comparison to PAO1, showed similar infection ability, however caused serious tissue necrosis effects, confirming the importance of hemolysins in tissue damage. Overall *in vivo* infection ability did not correlate well with the *in vitro* cytotoxicity, highlighting the importance of the animal models in this type of studies.

Due to the nature of data obtained in this study, the possibility to apply the state of the art an ensemble machine learning approach to assess the relative predictive importance of the cytotoxicity has been explored. This approach also highlighted submerged biofilm formation, as well as hemolysis, pyocyanin and swimming as good predictors of the cell-killing ability (Fig. 6). In order to build a reliable predictive model, it would be relevant to replicate similar studies in bigger samples of clinical and non-clinical populations of diverse origins and to include *in vivo* infection model data in the analysis. That effort could allow utilization of some of these phenotypic traits or specific combinations of thereof as useful prognostic markers or as novel targets for antimicrobial treatment.

While complex relationships between certain virulence factors are jet to be fully elucidated and understood, the general agreement is that virulence in *P. aeruginosa* is both multifactorial and combinatorial, and is the result of a pool of pathogenicity-related genes that interact in various combinations in different genetic backgrounds (Lee *et al*. 2006, Crousilles *et al*. 2015). However, given the importance of this pathogen and the fact that it is almost exclusively associated with difficult-to treat infections, identification of the reliable predictors of the infection ability is of great interest, and should be further addressed. In that sense, the machine self-learning approach that develops its knowledge

from the large datasets and builds predictions on continuous refinements is one of the possible ways ahead.

In summary, this study showed that animal *P. aeruginosa* isolates could be compared to human, all being phenotypically diverse and able to cause *in vitro* cell damage, as well as *in vivo* infections. Taken together, it also highlights the importance of pyocyanin-producing, biofilm-forming and hemolytic ability in pathogenesis of this strain. With a view of increased incidence of infections shared between pets and human handlers, and due to the fact that *P. aeruginosa* found its place in the latest WHO priority list of antibiotic-resistant bacteria (Tacconelli *et al.* 2018), this strain should be included in the more thorough surveillance and control efforts of veterinary clinics.

SUPPLEMENTARY DATA

Supplementary data are available at *FEMSPD* online.

ACKNOWLEDGEMENT

Dr Radmila Popović from the Regional Hospital Valjevo (Valjevo, Serbia) is acknowledged for human specimen collection and maintenance. Dr William Casey (UCD, Dublin, Ireland) is acknowledged for critical review of the manuscript.

FUNDING

This work was supported by the Ministry of Education, Science and Technological Development of Serbia (Grant No. 173048 and Grant No. 173001).

Conflict of interest. None declared.

REFERENCES

Arora SK, Neely AN, Blair B *et al.* Role of motility and flagellin glycosylation in the pathogenesis of *Pseudomonas aeruginosa* burn wound infections. *Infect Immun* 2005;**73**:4395–8.

Bodenhofer U, Klawonn F. Robust rank correlation coefficients on the basis of fuzzy orderings: initial steps. *Mathware Soft Comput* 2008;**15**:5–20.

Brannon MK, Davis JM, Mathias JR *et al.* *Pseudomonas aeruginosa* type III secretion system interacts with phagocytes to modulate systemic infection of zebrafish embryos. *Cell Microbiol* 2009;**11**:755–68.

Burchett WW, Ellis AR, Harrar SW *et al.* Nonparametric inference for multivariate data: The R package npmv. *J Stat Soft* 2017;**76**:18.

Chand NS, Lee JS, Clatworthy AE *et al.* The sensor kinase KinB regulates virulence in acute *Pseudomonas aeruginosa* infection. *J Bacteriol* 2011;**193**:2989–99.

Chen T, Guestrin C. *XGBoost: A Scalable Tree Boosting System. 22nd ACM SIGKDD International Conference on Knowledge Discovery and Data Mining*. San Francisco, CA, USA: ACM, 2016;785–94.

Clatworthy AE, Lee JS, Leibman M *et al.* *Pseudomonas aeruginosa* infection of zebrafish involves both host and pathogen determinants. *Infect Immun* 2009;**77**:1293–303.

Crousilles A, Maunders E, Bartlett S *et al.* Which microbial factors really are important in *Pseudomonas aeruginosa* infections? *Future Microbiology* 2015;**10**:1825–36.

Damborg P, Broens EM, Chomel BB *et al.* Bacterial zoonoses transmitted by household pets: State-of-the-art and future perspectives for targeted research and policy actions. *J Comp Pathol* 2016;**155**:S27–40.

Fernandez-Pinar R, Camara M, Dubern JF *et al.* The *Pseudomonas aeruginosa* quinolone quorum sensing signal alters the multicellular behaviour of *Pseudomonas putida* KT2440. *Res Microbiol* 2011;**162**:773–81.

Galili T. dendextend: an R package for visualizing, adjusting and comparing trees of hierarchical clustering. *Bioinformatics* 2015;**31**:3718–20.

Gellatly SL, Hancock RE. *Pseudomonas aeruginosa*: new insights into pathogenesis and host defenses. *Pathog Dis* 2013;**67**:159–73.

Ha D-G, Kuchma SL, O'Toole GA. Plate-based assay for swimming motility in *Pseudomonas aeruginosa*. In: Filloux A, Ramos J-L (eds) Pseudomonas Methods and Protocols. New York, NY: Springer, 2014a;59–65.

Ha D-G, Kuchma SL, O'Toole GA. Plate-based assay for swarming motility in *Pseudomonas aeruginosa*. In: Filloux A, Ramos J-L (eds) Pseudomonas Methods and Protocols. New York, NY: Springer, 2014b;67–72.

Haenni M, Hocquet D, Ponsin C *et al.* Population structure and antimicrobial susceptibility of *Pseudomonas aeruginosa* from animal infections in France. *BMC Vet Res* 2015;**11**:9.

Hauser AR. *Pseudomonas aeruginosa*: So many virulence factors, so little time. *Crit Care Med* 2011;**39**:2193–4.

Hillier A, Alcorn JR, Cole LK *et al.* Pyoderma caused by *Pseudomonas aeruginosa* infection in dogs: 20 cases. *Vet Dermatol* 2006;**17**:432–9.

Kidd TJ, Gibson JS, Moss S *et al.* Clonal complex *Pseudomonas aeruginosa* in horses. *Vet Microbiol* 2011;**149**:508–12.

Kieser M, Friede T, Gondan M. Assessment of statistical significance and clinical relevance. *Statist Med* 2013;**32**:1707–19.

Kumar S, Stecher G, Tamura K. MEGA7: Molecular Evolutionary Genetics Analysis Version 7.0 for Bigger Datasets. *Mol Biol Evol* 2016;**33**:1870–4.

Lau GW, Hassett DJ, Ran H *et al.* The role of pyocyanin in *Pseudomonas aeruginosa* infection. *Trends Mol Med* 2004;**10**:599–606.

Lee DG, Urbach JM, Wu G *et al.* Genomic analysis reveals that *Pseudomonas aeruginosa* virulence is combinatorial. *Genome Biol* 2006;**7**:R90.

Lee K, Yoon SS. *Pseudomonas aeruginosa* Biofilm, a programmed bacterial life for fitness. *J Microbiol Biot* 2017;**27**:1053–64.

Li G, Peng H, Zhang J *et al.* Robust rank correlation based screening. *Ann Statist* 2012;**40**:1846–77.

Lister PD, Wolter DJ, Hanson ND. Antibacterial-resistant *Pseudomonas aeruginosa*: clinical impact and complex regulation of chromosomally encoded resistance mechanisms. *Clin Microbiol Rev* 2009;**22**:582–610.

Llamas MA, van der Sar A, Chu BC *et al.* A novel extracytoplasmic function (ECF) sigma factor regulates virulence in *Pseudomonas aeruginosa*. *PLoS Pathog* 2009;**5**:e1000572.

Loeffler A, Lloyd DH. Companion animals: a reservoir for methicillin-resistant *Staphylococcus aureus* in the community? *Epidemiol Infect* 2010;**138**:595–605.

Mahajan-Miklos S, Tan M-W, Rahme LG *et al.* Molecular mechanisms of bacterial virulence elucidated using a *Pseudomonas aeruginosa*– *Caenorhabditis elegans* pathogenesis model. *Cell* 1999;**96**:47–56.

Merritt JH, Kadouri DE, O'Toole GA. Growing and analyzing static biofilms. *Curr Protocol Microbiol* 2005, DOI: 10.1002/9780471729259.mc01b01s00.

Mittal R, Sharma S, Chhibber S *et al.* Correlation between serogroup, *in vitro* biofilm formation and elaboration of virulence factors by uropathogenic *Pseudomonas aeruginosa*. *FEMS Immunol Med Mic* 2010;**58**:237–43.

O'Loughlin CT, Miller LC, Siryaporn A *et al.* A quorum-sensing inhibitor blocks *Pseudomonas aeruginosa* virulence and biofilm formation. *Proc Natl Acad Sci USA* 2013;**110**: 17981–6.

Oglesby-Sherrouse AG, Djapgne L, Nguyen AT *et al.* The complex interplay of iron, biofilm formation, and mucoidy affecting antimicrobial resistance of *Pseudomonas aeruginosa*. *Pathog Dis* 2014;**70**:307–20.

Ohnishi M, Sawada T, Hirose K *et al.* Antimicrobial susceptibilities and bacteriological characteristics of bovine *Pseudomonas aeruginosa* and *Serratia marcescens* isolates from mastitis. *Vet Microbiol* 2011;**154**:202–7.

Olejnickova K, Hola V, Ruzicka F. Catheter-related infections caused by *Pseudomonas aeruginosa*: virulence factors involved and their relationships. *Pathog Dis* 2014;**72**:87–94.

Pereira SG, Rosa AC, Ferreira AS *et al.* Virulence factors and infection ability of *Pseudomonas aeruginosa* isolates from a hydropathic facility and respiratory infections. *J Appl Microbiol* 2014;**116**:1359–68.

Petersen AD, Walker RD, Bowman MM *et al.* Frequency of isolation and antimicrobial susceptibility patterns of *Staphylococcus intermedius* and *Pseudomonas aeruginosa* isolates from canine skin and ear samples over a 6-year period (1992-1997). *J Am Anim Hosp Assoc* 2002;**38**:407–13.

Pye CC, Yu AA, Weese JS. Evaluation of biofilm production by *Pseudomonas aeruginosa* from canine ears and the impact of biofilm on antimicrobial susceptibility in vitro. *Vet Dermatol* 2013;**24**:446–49, e498-49.

Scaccabarozzi L, Leoni L, Ballarini A *et al.* *Pseudomonas aeruginosa* in dairy goats: Genotypic and phenotypic comparison of intramammary and environmental isolates. *PLoS One* 2015;**10**:e0142973.

Stover CK, Pham XQ, Erwin AL *et al.* Complete genome sequence of *Pseudomonas aeruginosa* PAO1, an opportunistic pathogen. *Nature* 2000;**406**:959–64.

Streeter K, Katouli M. *Pseudomonas aeruginosa*: A review of their pathogenesis and prevalence in clinical settings and the environment. *Infect Epidemiol Med* 2016;**2**:25–32.

Tacconelli E, Carrara E, Savoldi A *et al.* Discovery, research, and development of new antibiotics: the WHO priority list of antibiotic-resistant bacteria and tuberculosis. *Lancet Infect Dis* 2018;**18**:318–27.

Trøstrup H, Lerche CJ, Christophersen LJ *et al.* Chronic *Pseudomonas aeruginosa* biofilm infection impairs murine S100A8/A9 and neutrophil effector cytokines—implications for delayed wound closure? *Pathog Dis* 2017;**75**:ftx068-.

Vives-Florez M, Garnica D. Comparison of virulence between clinical and environmental *Pseudomonas aeruginosa* isolates. *Int Microbiol* 2006;**9**:247–52.

Wright EA, Di Lorenzo V, Trappetti C *et al.* Divergence of a strain of *Pseudomonas aeruginosa* during an outbreak of ovine mastitis. *Vet Microbiol* 2015;**175**:105–13.